MAGNETIC SUSCEPTIBILITY MEASUREMENTS ON $CsTi(SO_4)_2 \cdot 12H_2O$

by

James Leonard Bickerton

A thesis submitted
to the Board of Graduate Studies
in partial fulfilment of the requirements
for the degree of
Master of Science

Solid State Laboratory
Physics Department
Sir George Williams University
Montreal
August 1969

ABSTRACT

MAGNETIC SUSCEPTIBILITY MEASUREMENTS ON

$CsTi(SO_4)_2.12H_2O$

by

James Leonard Bickerton

The magnetic susceptibility of powdered samples of CsTi Alum ($CsTi(SO_4)_2.12H_2O$) was studied in the temperature range from room temperature to liquid helium temperature. The theory of H. Kamimura (1956) was used to calculate the theoretical magnetic susceptibility as a function of two parameters, $x=-\bar{r^2}A/7kT$ and $y=\lambda/2kT$. A is the coefficient of the trigonal field and λ is the spin-orbit coupling constant. The best fit of the experimental results to the theory was obtained for $\lambda=25.2\pm2.5$ cm^{-1} and $\bar{r^2}A=-36.6\pm3.5$ cm^{-1}. Using these results, the energy levels of the three lowest Kramers' doublets were calculated to be:

$$E_1^{(0)}= -2.1 \text{ cm}^{-1}$$
$$E_2^{(0)}= 29.4 \text{ cm}^{-1}$$
$$E_3^{(0)}=-27.3 \text{ cm}^{-1}$$

The magnetic susceptibility results reported here are in good agreement with the results of Dutta-Roy et al.(1959), and Figgis et al.(1963). Also the value obtained for the low lying excited state is in good agreement with the value predicted by Van Vleck (1940), and calculated by Bleaney et al.(1955).

TABLE OF CONTENTS

ACKNOWLEDGEMENTS

The author wishes to thank Dr. J.A. MacKinnon for suggesting this thesis problem and for his constant encouragement during the course of the research. In addition, the author is grateful to Dr. R.C. Sharma for his encouragement and helpful advice.

The author also acknowledges the assistance of Mr. J. Blaison and his staff in some of the experimental aspects of the research. A special note of thanks to Mr. J. Lousteau for his helpful assistance in the construction of a glove box.

Finally, gratitude must be expressed to the National Research Council of Canada for financial assistance in the form of one Scholarship.

ABSTRACT

The magnetic susceptibility of powdered samples of $CsTi(SO_4)_2 \cdot 12H_2O$ was studied in the temperature range from $300^\circ K$ to $4.2^\circ K$. The curve of magnetic susceptibility versus 1000/T deviated from a straight line at approximately $25^\circ K$.

The theory of H. Kamimura (1956) was used to calculate the theoretical magnetic susceptibility as a function of two parameters, $x = -\overline{r^2}A/7kT$ and $y = \lambda/2kT$. A is the coefficient of the trigonal field and λ is the spin-orbit coupling constant. The best fit of the experimental results to the theory was obtained for $\lambda = 25.2 \pm 2.5$ cm^{-1} and $\overline{r^2}A = -36.6 \pm 3.5$ cm^{-1}. Using these results, the energy levels of the three lowest Kramers' doublets were calculated with respect to the degenerate $d\varepsilon^{(1)}$ orbital before splitting.

$$E_1^{(0)} = -2.1 \text{ cm}^{-1}$$
$$E_2^{(0)} = 29.4 \text{ cm}^{-1}$$
$$E_3^{(0)} = -27.3 \text{ cm}^{-1}$$

The magnetic susceptibility results reported here are in good agreement with the results of Dutta-Roy et al.(1959), and Figgis et al.(1963). Also the value obtained for the low lying excited state is in good agreement with the value predicted by Van Vleck (1940), and the value calculated by Bleaney et al.(1955).

INTRODUCTION

The magnetic properties of CsTi Alum ($CsTi(SO_4)_2 \cdot 12H_2O$) have been of interest ever since the first experiments were done on the material by de Haas and Wiersma in 1935. Since then, magnetic susceptibility experiments have been performed by Kurti and Simon (1935), Van den Handel (1940), Benzie and Cooke (1951), Dutta-Roy et al. (1959), and Figgis et al. (1963). Closely related to these experiments are the electron paramagnetic resonance experiments performed by Bleaney et al. (1955). The results of all these experiments show that there is a decrease in the effective magnetic moment as the temperature of the sample is lowered from 300°K to 4.2°K. Because of a lack of experimental data in the liquid nitrogen to liquid helium temperature range, it is difficult to establish where the transition occurs and whether the change is a smooth or abrupt one.

The object of this research is to obtain magnetic susceptibility measurements on CsTi Alum in the temperature region from 300°K to 4.2°K, with particular emphasis on the liquid nitrogen to liquid helium temperature range.

CHAPTER 1

HISTORY OF EXPERIMENTS ON $CsTi(SO_4)_2 \cdot 12H_2O$

The experimental research done on paramagnetic ions of the iron group has quickly grown since the first experiments were performed on these materials in the mid 1930's. Titanium three plus, with a single 3d electron about an inert argon core and a ^2D ground state orbital term, should be one of the most studied and best understood ions of the group. But this is not the case. From the outset, there has been a lack of experimental data about the trivalent titanium ion. The reason for this lack of data is the difficulty in preparing and preserving the titanium compounds. In an oxygen atmosphere titanium three plus oxidizes to the more stable four plus state, forming in the process the diamagnetic material TiO_2.

In 1935, de Haas and Wiersma did some adiabatic demagnetization experiments on CsTi Alum, and found that it obeyed a Curie law in the liquid helium temperature range. The agreement between theory and experiment was poor due to the fact that the spectroscopic splitting factor "g" was assumed to be two, when in fact it was considerably less than two. Van den Handel (1940) measured the mean magnetic susceptibility of four different samples of CsTi Alum in

the temperature region from 300°K to 4.2°K but, a meaningful interpretation was difficult because of an inconsistency in his results.

Benzie and Cooke (1951) recorded magnetic susceptibility measurements on powdered samples of the Alum in the temperature region from 4.2°K to 1.0°K. The susceptibility was found to obey a Curie law with a mean Curie constant of 0.118/mole, corresponding to a "g" value of 1.12.

Dutta-Roy et al. (1959) reported detailed magnetic susceptibility measurements on single crystals of CsTi Alum throughout the temperature range 300°K to 100°K. Bose et al. (1959), using crystal field theory and assuming a trigonal field splitting of 800 cm^{-1}, were able to obtain good agreement with the results of Dutta-Roy et al. Bose's calculations gave "g" parallel equal to 1.919 and "g" perpendicular equal to 1.775. These results were difficult to reconcile with the results of the EPR experiments performed at liquid helium temperature by Bleaney et al. (1955). Bleaney's group calculated "g" parallel equal to 1.250 and "g" perpendicular equal to 1.140, corresponding to a trigonal field splitting of 50 cm^{-1}.

To explain the very short spin-lattice relaxation time (10^{-7}sec.) of CsTi Alum at liquid nitrogen temperature obtained by Gorter et al. (1938), Van Vleck (1940) assumed a Raman process as the mechanism of spin-lattice relaxation. In this temperature range, the trigonal field splitting was

in the order of 1000 cm^{-1}. To explain the relaxation time of 10^{-3} sec. in the liquid helium temperature region obtained by de Haas and du Pré in 1938, Van Vleck still assumed a Raman process but the trigonal field splitting was reduced to 100 cm^{-1}. Bose et al. (1959) suggested that there was a transition in the effective magnetic moment at some temperature between 300°K and 4.2°K that would explain the large discrepancy in the observed results.

Figgis et al. (1963) measured the magnetic susceptibility of CsTi Alum in the temperature region from 300°K to 80°K. Their results were in disagreement with some of the earlier findings in that they found the trigonal field splitting equal to 350 cm^{-1}. They, however, did conclude that their value could not explain the entire temperature range.

This short history on the magnetic susceptibility of CsTi Alum indicates that until more experimental data for the entire temperature range is obtained, it will be difficult to explain the large discrepancy in the observed results.

CHAPTER 2

THEORY

The purpose of this chapter is to discuss briefly the basic topics in the study of Ti^{3+} ion in a crystal lattice under the influence of an external magnetic field.

2.1 Hamiltonian of the free Titanium ion

When an ion is placed in a crystal lattice, the energy levels of the ion are modified by the crystal surroundings. In order to understand these modifications, it is important to review the interactions involved with a free ion.

The most important interaction in an atom is the Coulomb interaction V_f. This term consists of the interaction of the electrons with the nuclear charge Ze, and the mutual repulsion of the electrons.

The next important interaction is a magnetic interaction V_{ls}, between the electron spins with the orbital angular momentum. If the system is confined to Russell-Saunders coupling, the spin-orbit interaction can be expressed as $\lambda L.S$ where λ is the spin-orbit coupling parameter for a given ion. A much weaker spin-spin interaction V_{ss} takes into account the mutual interaction between the magnetic dipoles.

If the nucleus has a spin I and a quadrupole moment Q, two additional interactions must be considered. The first is the interaction V_n between the nuclear moment

and the magnetic moments of the electron. The second addition V_q is the electrostatic interaction with the quadrupole moment Q of the nucleus.

The free ion Hamiltonian is then given by the sum of these interactions.

$$H = V_f + V_{ls} + V_{ss} + V_n + V_q \qquad 2.1$$

The order of magnitude of these interactions can be estimated from the observed atomic spectra. $V_f \sim 10^5$ cm^{-1}, whereas $V_{ls} \sim 10^2$ cm^{-1} for the iron group and 10^3 cm^{-1} for the rare earths and uranium group; $V_{ss} \sim 10^0$ cm^{-1}, $V_n \sim 10^{-1}$ cm^{-1} to 10^{-3} cm^{-1}, and $V_q \sim 10^{-3}$ cm^{-1}.

2.2 Hamiltonian of trivalent Titanium in a crystal lattice

When an ion is placed in a crystal lattice, additional terms representing the effects of the lattice on the motion of the electrons must be introduced in the Hamiltonian for the free ion. In the case of $CsTi(SO_4)_2 \cdot 12H_2O$, the nearest neighbours are the six water dipoles. They are arranged about the titanium ion in a near octahedral configuration with the negative ends of the dipoles pointing towards the titanium ion. These water dipoles give rise to a crystalline electric field at the titanium site that is of dominantly cubic symmetry. The deviation from the cubic symmetry is provided by the Jahn-Teller effect and the indirect action of the field from distant atoms. Because of the Jahn-Teller effect, the $6H_2O$ molecules will always arrange themselves around the titanium ion in such a way

that the latter is a nondegenerate state if there is stability. Consequently, if a cubic field yields a degenerate state for the titanium ion, the water cluster will warp itself, even without disturbing influences from distant atoms, so that it is no longer octahedrally arranged. Thus the crystal field partially lifts the fivefold orbital degeneracy of the ^2D ground state. The result is a triplet state and a doublet state with the triplet lying lowest. The triplet is labelled the $d\varepsilon^{(1)}$ orbital and the doublet the $d\gamma^{(1)}$ orbital with a separation of the two orbitals labelled 10Dq. For CsTi Alum, the separation is of the order of 20,000 cm^{-1}.

The threefold degenerate $d\varepsilon^{(1)}$ orbital splits into three Kramers' doublets (degenerate in spin only) when a trigonal field and spin-orbit interaction are taken into account. The $d\gamma^{(1)}$ orbital is also split by the same interactions into two Kramers' doublets. In both orbitals the trigonal field and spin-orbit interactions are about equal in magnitude. At liquid helium temperature only the lowest Kramers doublet is populated appreciably, since the next highest doublet is separated by more than kT. To remove the Kramers degeneracy, an external magnetic field must be applied. See figure # 2 for the energy level diagram of CsTi Alum in the absence of an external magnetic field.

2.3 Magnetism and Magnetic Susceptibility

All magnetic effects are due to magnetic moments $\vec{u}$, through their interaction with each other and with an external magnetic field. When a particular material is placed in an external magnetic field, the collective effect of all the individual magnetic moments is defined as the magnetization $\vec{M}$. The ratio of this quantity to the magnetic field $\vec{H}$ is defined as the magnetic susceptibility X of the material.

In all materials, orbiting electrons give rise to magnetic moments. Under the influence of an external magnetic field, these moments tend to align themselves against the field, giving a negative susceptibility. This is the origin of diamagnetism, the effect of which is always present when a material is placed in a magnetic field. This effect is temperature independent.

Some atoms have permanent magnetic moments which tend to align themselves in a magnetic field. This effect, called paramagnetism, gives rise to a positive susceptibility. Paramagnetism is different from diamagnetism in that the individual moments arise from unpaired electron spins which are not affected by the diamagnetic influence. The orbiting electrons present produce diamagnetism, but it is usually negligible with respect to the paramagnetism.

The tendency for the magnetic moments to align themselves with the external field is affected by thermal agitation.

The temperature dependence of paramagnetism is expressed by Curie's law

$$X = C/T \qquad 2.2$$

where C is the Curie constant.

A theoretical basis for this law is provided by Langevin's classical approach to a system of N magnetic moments $\vec{u}$ where

$$X = Nu^2/3kT \qquad 2.3$$

for $uH \ll kT$.

By using a quantum mechanical approach to the system of moments based on the quantization of the total angular momentum $\vec{J}$ of the ion or atom in question, a more useful result is obtained.

$$X = g^2B^2NJ(J+1)/3kT \qquad 2.4$$

B is the Bohr magneton and g is the Landé spectroscopic splitting factor.

Kamimura, using Van Vleck's formula for susceptibility calculated the effective magnetic moment for a $d\varepsilon^{(1)}$ manifold. Using equation 2.5, Kamimura's results can be used to calculate the effective magnetic moment for powdered samples of CsTi Alum.

$$u^2_{eff(av)} = \frac{1}{3} u^2_{eff(\parallel)} + \frac{2}{3} u^2_{eff(\perp)} \qquad 2.5$$

where $u^2_{eff(\parallel)}$ and $u^2_{eff(\perp)}$ are given by equations 2.6 and 2.7 respectively.

$$u^2_{eff(//)} = \left\{ 3 \left\{ \frac{4y^2}{3C-(6x+y)C^{1/2}} - 1 \right\}^2 - \frac{4y^2}{C^{3/2}} \right.$$

$$\left. + \left[3 \left\{ \frac{4y^2}{3C+(6x+y)C^{1/2}} - 1 \right\}^2 + \frac{4y^2}{C^{3/2}} \right] \exp(3C^{1/2}) \right\}$$

$$\times \left(1 + \exp(3C^{1/2}) + \exp(-3x+\tfrac{3}{2}y+\tfrac{3}{2}C^{1/2}) \right)^{-1} \qquad 2.6$$

$$u^2_{eff(\perp)} = \frac{3}{1+\exp(3C^{1/2}) + \exp(-3x+\frac{3}{2}y+\frac{3}{2}C^{1/2})} \times$$

$$\left[2 \left\{ \frac{4x^2-\frac{4}{3}xy+y^2 - (2x-y)C^{1/2}}{(-2x+y+C^{1/2})(3C-(6x+y)C^{1/2})} + \right.\right.$$

$$\left.\left. \frac{4x^2-\frac{4}{3}xy+y^2 + (2x-y)C^{1/2}}{(-2x+y-C^{1/2})(3C+(6x+y)C^{1/2})} \right\} \exp(-3x+\tfrac{3}{2}y+\tfrac{3}{2}C^{1/2}) \right.$$

$$+ \left\{ \left(\frac{12x^2+y^2+(6x-y)C^{1/2}}{3C+(6x+y)C^{1/2}} \right)^2 + \frac{(2x+y)^2}{3C^{3/2}} \right.$$

$$- 2 \frac{4x^2-\frac{4}{3}xy+y^2+(2x-y)C^{1/2}}{(-2x+y-C^{1/2})(3C+(6x+y)C^{1/2})} \exp(3C^{1/2})$$

$$+ \frac{12x^2+y^2-(6x-y)C^{1/2}}{3C-(6x+y)C^{1/2}}^2 - \frac{(2x+y)^2}{3C^{3/2}}$$

$$- 2 \frac{4x^2-\frac{4}{3}xy+y^2-(2x-y)C^{1/2}}{(-2x+y+C^{1/2})\ (3C-(6x+y)C^{1/2})} \qquad 2.7$$

where $C = 4x^2 + \frac{4}{3}xy + y^2$, $x = -\overline{r^2}A/7kT$ and $y = \lambda/2kT$.

$\overline{r^2} = \int (f(r))^2 r^4 dr$ where $f(r)$ is the radial part of the wave function. A is the coefficient of the trigonal field and λ is the spin-orbit coupling parameter. The magnetic susceptibility (emu/gm) for any temperature T can be calculated from equation 2.8, where $u_{eff(av)}$ is in Bohr magnetons and N is the number of molecules per gram.

$$X = \frac{Nu^2_{eff(av)}}{3kT} \qquad 2.8$$

Kamimura derived the expressions for the energy levels of the three Kramers' doublets of the $d\varepsilon^{(1)}$ manifold as a function of λ and $\overline{r^2}A$. Assuming A to be negative, the ground state of CsTi Alum is given by $E_3^{(0)}$.

The energy levels of the three lowest Kramers' doublets are:

$$E_1^{(0)} = -\frac{2}{7}\overline{r^2}A - \frac{1}{2}\lambda \qquad 2.9$$

$$E_2^{(0)} = \frac{1}{7}\overline{r^2}A + \frac{1}{4}\lambda + \frac{3}{2}\left[\frac{4}{49}(\overline{r^2}A)^2 - \frac{2}{21}\lambda\overline{r^2}A + \frac{1}{4}\lambda^2\right]^{1/2} \qquad 2.10$$

$$E_3^{(0)} = \frac{1}{7}\overline{r^2}A + \frac{1}{4}\lambda - \frac{3}{2}\left[\frac{4}{49}(\overline{r^2}A)^2 - \frac{2}{21}\lambda\overline{r^2}A + \frac{1}{4}\lambda^2\right]^{1/2} \qquad 2.11$$

CHAPTER 3

EXPERIMENTAL APPARATUS AND PROCEDURE

3.1 Sample preparation

The crystals of CsTi Alum were grown by Dr. Fredrick of the Chemistry department of McGill University. To eliminate the problem of oxidation of the samples, the crystals were stored under a nitrogen atmosphere in a glove box built by the author. When measurements were to be made on the sample, it was crushed into powdered form and packed into the sample holder. This operation was performed in the glove box so that the sample would not be exposed to the oxygen atmosphere. The sample holder was then removed from the glove box and weighed before attaching it to the sample rod assembly. Knowing the weight of the sample holder without a sample in it, the weight of the sample of CsTi Alum was determined.

The samples of CsTi Alum were studied in powdered form for the following reasons:

1. Since the crystal structure of CsTi Alum is cubic, the magnetic susceptibility is isotropic.
2. A method of gluing large single crystals on the end of the sample holder failed due to the fact that the glue lost its adhesive properties at the low temperatures involved in the experiment.

3. A method of placing small single crystals in the sample holder was discarded because it was impossible to know whether the crystals were stationary relative to the sample holder.
4. For accurate measurements of the magnetic moment of the sample, it was essential that the CsTi Alum sample and the nickel sample used for the calibration had the same position with respect to the Z axis. See figure on next page.

3.2 Calibration of magnetometer

The magnetometer was calibrated at room temperature using a standard nickel sample provided by the Princeton Applied Research Company. The saturation magnetization of this nickel sample was 54.39 emu/gm.

When the nickel sample was located symmetrically with respect to the detection coils, it was at a " saddle point " with respect to the coil output voltage. That is, the coil output voltage was simultaneously a maximum for displacement of the sample along the Z or X axis, and a minimum for displacement along the Y axis. See figure on next page. The sample rod assembly was adjusted in the X, Y, and Z directions independently of each other to locate the " saddle point ". When making the adjustments, it was important that the Z adjustment be made first, since, if the Z adjustment was "off" sufficiently, the other adjustments

would not "peak" properly. However, regardless of the X and Y settings, within the limits of the fine adjustment provided, a maximum was always obtained for Z.

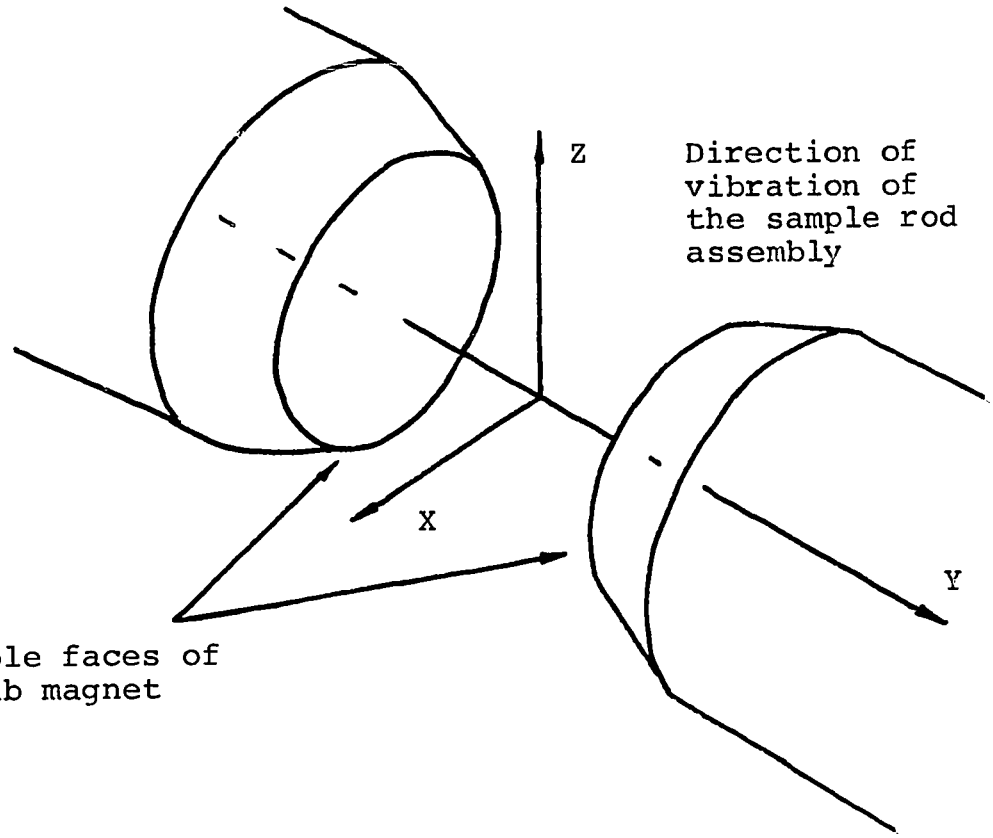

3.3 Calibration of thermocouple

A copper-constantan thermocouple with the reference junction immersed in a liquid helium bath, was used to measure the temperature of the sample. A calibration[29] was used to obtain the temperatures corresponding to the various observed thermocouple emf's. When both junctions of the thermocouple were at liquid helium temperature, a small emf was observed. This value changed from day to day, due to thermal and contact emf's. The thermocouple emf's observed during an experiment were corrected for

these stray emf's before the thermocouple calibration was applied. To interpolate between the calibration points, a curve fit program was used.

3.4 Calibration of magnetic field

A Varian Model 3603 12" electromagnet was used to provide the magnetic field for the experiment. The magnet was calibrated in the region from 1 k-gauss to 20 k-gauss using a Varian Model F-8A nuclear fluxmeter. By monitoring the transmitter frequency of the fluxmeter with an electronic counter, the magnetic field was calculated to within ± 0.05 gauss. The field was calibrated in two ranges. To obtain the corrected field, the frequency of the counter was multiplied by a constant that depended on the calibration probe used. The details of the calibration are given in the table below. For the calibration curve of the electromagnet, see figure # 3.

Field Range (k-gauss)	Calibration Probe	Calculated Field (k-gauss)
1 - 8	Proton	H = .2349 x f
8 - 20	Deuteron	H =1.5299 x f

The frequency of the counter is measured in megacycles.

3.5 Experimental procedure

When a sample of magnetic material is placed in a uniform magnetic field, the field in the neighbourhood of

the sample will consist of the original uniform field plus a non-uniform field due to the sample. The strength of this field is a measure of the sample magnetization and hence its susceptibility. The vibrating sample magnetometer used for this research operates by detecting and measuring the part of the field due to the sample. The electronic detection system of the magnetometer is designed such that the output signal represents the magnetic moment of the sample on the relative linear magnetic moment scale defined by the system. See figure # 1 for a block diagram of the experiment. For a detailed treatment of the detection system, see appendix 1.

The magnetic moment of CsTi Alum was measured in the temperature region from 300°K to 4.2°K, with emphasis on the liquid nitrogen to liquid helium temperature range. To obtain temperatures above 4.2°K, a heater, built into the tail section of the Andonian liquid helium dewar, was used. The flow of liquid helium to the sample chamber was held constant. For each temperature recorded, the sample signal was measured as a function of the magnetic field. The entire range of the magnet was used in both the forward and reverse directions. The analysis of the data was done on a C.D.C. 3300 digital computer. A summary of the analysis is as follows.

1. The magnetic fields and temperatures were calculated using the respective calibrations.
2. The slope of the curve of sample signal versus magnetic field was obtained and a corrected set

of sample signals was generated. These signals were converted to magnetic moments (emu) by multiplying by the nickel calibration constant for the day of the experiment.

3. The sample holder signal, which was found to be a function of the magnetic field H, and the temperature T, is given by equation 3.1.

$$Sig(T,H) = (A+BT+CT^2)xH \qquad 3.1$$

where $A = 1.667x10^{-3}$

$B = -8.015x10^{-5}$

$C = 7.604x10^{-7}$

This value was multiplied by the calibration constant for the day the experiment was performed on the sample holder. This final sample holder correction was subtracted from the magnetic moments in step 2 above.

4. The corrected magnetic moments in step 3 above were divided by the mass of the sample for the day of the experiment to give the magnetic moment in units of emu/gm. The magnetic susceptibility was obtained by finding the slope of the curve of magnetic moment (step 4) versus magnetic field. The diamagnetism of the lattice was added to the magnetic susceptibility.[26]

5. The theory of H. Kamimura (1956) was used to calculate the theoretical magnetic moment and hence the magnetic susceptibility as a function of two parameters,

The least square criterion was used to obtain the best fit of the experimental data to the theory. The energy levels of the $d\epsilon^{(1)}$ manifold were calculated as a function of λ and $\overline{r^2}A$.

TABLE # 1

List of Experimental Apparatus and their Manufacturer

	Instrument	Manufacturer
1.	Vibrating sample magnetometer	Princeton Applied Research Company
2.	Model 3603 electro-magnet	Varian Associates
3.	Liquid helium dewar	Andonian Associates
4.	Nuclear fluxmeter	Varian Associates
5.	Digital voltmeter	John Fluke Company
6.	Electronic counter	Hewlett-Packard

CHAPTER 4

RESULTS AND DISCUSSION

The effective magnetic moment of several powdered samples of CsTi Alum is obtained as a function of temperature. The experimental results are shown in table # 2 on the next page. Figure # 5 shows the effective magnetic moment as a function of temperature. Figure # 6 is a plot of the magnetic susceptibility versus 1000/T. In both graphs, the curve represents the best fit of the experimental data to the theory of H. Kamimura (1956). The best fit is obtained for the following values of the two running parameters.

$$\overline{r^2}A = -36.6 \pm 3.5 \text{ cm}^{-1}$$

$$\lambda = 25.2 \pm 2.5 \text{ cm}^{-1}$$

The energy levels of the three lowest Kramers' doublets are calculated as a function of these two parameters. The results are shown in Fig. #7. In this calculation, the energy level splitting is independent of the temperature. As the temperature of the sample is lowered, one would expect the magnitude of the trigonal field parameter A and the spin-orbit coupling parameter λ to change. The exact manner in which these parameters change with temperature, if at all, is difficult to determine at this time.

Table # 2

Magnetic Susceptibility of

$CsTi(SO_4)_2 \cdot 12H_2O$

T	1000/T	u_{eff} (exp)	X (exp)
^oK	$^oK^{-1}$	Bohr Magnetons	10^{-6} emu/gm
Results-April 9,1969.			
17.	59.2	1.36	23.1
30.	33.3	1.81	23.3
52.	19.4	2.00	16.5
64.	15.7	2.01	13.5
78.	12.8	2.10	12.0
14.	71.4	1.24	23.3
21.	47.8	1.51	23.1
26.	37.9	1.71	23.5
40.	24.8	1.93	19.7
4.2	238.	1.10	61.0
Results-April 11,1969.			
4.2	238.	1.06	56.9
14.	70.4	1.22	22.2
21.	47.2	1.41	20.1
30.	33.0	1.68	19.8
40.	24.8	1.73	15.7
51.	19.8	1.79	13.4

T ^{o}K	1000/T $^{o}K^{-1}$	u_{eff} (exp) Bohr Magnetons	X (exp) 10^{-6} emu/gm
60.	16.8	1.77	11.2
70.	14.2	1.83	10.1
81.	12.4	1.84	8.9
91.	11.0	1.90	8.4
101.	9.9	1.88	7.5
11.	93.5	1.12	24.7
295.	3.4	2.30	3.8
Results-June 5,1969.			
28.	36.1	1.84	26.1
16.	64.5	1.24	21.2
10.	100.0	1.29	34.9
13.	78.7	1.24	25.7
15.	66.6	1.32	24.2
18.	55.5	1.42	23.9
20.	50.0	1.52	23.8
24.	42.2	1.67	25.1
26.	38.3	1.78	25.9
33.	29.9	1.92	23.4
41.	24.4	1.83	17.3
53.	19.0	1.85	13.9
61.	16.3	2.11	15.4

The use of a low lying excited state to explain the experimental behavior of CsTi Alum is not new. Van Vleck (1940) suggested this theory as a possible solution to the very rapid spin-lattice relaxation times observed in CsTi Alum at liquid helium and liquid nitrogen temperatures.

The experimental results reported here are in good agreement with the high temperature range (300° K to 100° K) magnetic susceptibility results of Dutta-Roy et al. (1959), Figgis et al. (1963), and with the low temperature (4.2° K) EPR results reported by Bleaney et al. (1955). Also the calculated value of the low lying excited state is of the same order of magnitude as the value (100 cm^{-1}) predicted by Van Vleck in 1940, and value (50 cm^{-1}) calculated by Bleaney et al. (1955).

The excellent agreement between theory and experiment is achieved at the expense of a substantial reduction in the spin-orbit coupling parameter λ. This large reduction in λ from the free ion value (154 cm^{-1}) might not be so difficult to reconcile in the light of the large amount of covalent bonding which appears to be present in CsTi Alum.

CHAPTER 5

CONCLUSION

The primary object of this research which was to obtain magnetic susceptibility measurements on CsTi Alum ($CsTi(SO_4)_2.12H_2O$) in the temperature range from 300°K to 4.2°K, with emphasis on the liquid nitrogen to liquid helium temperature range, was achieved.

The application of the theory of H. Kamimura to the experimental results gave excellent agreement for one set of parameters that covered the entire temperature range studied. The calculated results are:

$$\overline{r^2}A = -36.6 \text{ cm}^{-1} \pm 3.5 \text{ cm}^{-1}$$

$$\lambda = 25.2 \text{ cm}^{-1} \pm 2.5 \text{ cm}^{-1}$$

$$E_1^{(0)} = -2.1 \text{ cm}^{-1}$$

$$E_2^{(0)} = 29.4 \text{ cm}^{-1}$$

$$E_3^{(0)} = -27.3 \text{ cm}^{-1}$$

The magnetic susceptibility results reported here are in good agreement with the results of Dutta-Roy et al.(1959) and Figgis et al.(1963). Also the value obtained for the low lying excited state is in good agreement with the value predicted by Van Vleck (1940), and the value calculated by Bleaney et al.(1955).

APPENDIX 1

DETECTION SYSTEM OF THE MAGNETOMETER

The Princeton Applied Research vibrating sample magnetometer is based on an instrument first described by S.Foner.[16] Figure # 4 is a functional diagram of the electronic system. The operating system of the magnetometer, as described in the reference manual supplied with the apparatus, is as follows (numbers in parenthesis refer to figure # 4):

The sample is suspended by a long vertical rod which is vibrated vertically by a transducer. Attached to the rod is a pair of circular metal plates, which along with a pair of fixed plates make up a vibrating capacitor assembly.

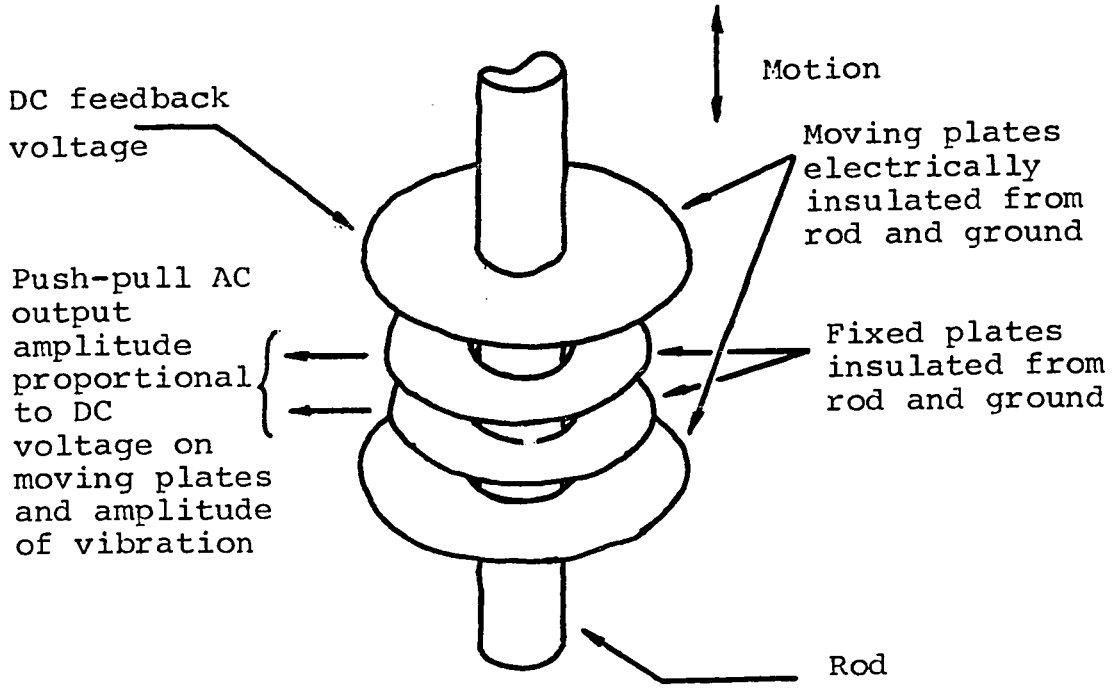

The sample and the detection coils are in an externally generated magnetic field, the sample moving relative to the field, the detection coils being stationary in it. Under these conditions an A.C. signal at the vibration frequency whose amplitude is proportional to the magnetic moment of the sample is generated in the detection coils. This signal is applied to the "sample signal input" of the electronic system (3). A signal of the same frequency appears between the fixed plates of the vibrating capacitor assembly. This signal, whose amplitude is proportional to the D.C. voltage applied to the moving plates, is applied to the "reference signal input" (2) of the electronic system. After passing through a pre-amplifier (6), a variable phase shifter (7), and a variable attenuator (8), the signal is combined with the sample signal in the primary of summing transformer (10). If the two inputs to the transformer are equal in magnitude and in-phase, the output of the secondary will be zero. The phase of the sample signal is primarily determined by the phase of the mechanical motion of the system. The phase of the reference signal is determined primarily by the phase of the mechanical motion, a small adjustment being provided by phase shifter (7). Consequently, for a given setting of attenuator (8), and with a proper adjustment of phase shifter (7), there is a definite value of D.C. feedback voltage at (4) for which the transformer output will be zero. If the reference signal

is too large there will be an output from the transformer; if it is too small there will also be an output but with the opposite phase.

The output of the transformer is fed via variable gain amplifier (9) to phase sensitive detector (17). The output of this detector is a D.C. voltage proportional to the amplitude of the transformer, whose polarity depends on the phase of the transformer, i.e., on whether the sample or reference signal is larger. This D.C. signal is fed through low-pass amplifier (16) which determines the noise bandwidth of the system and which also provides the high D.C. output voltage swings (0 to 90 volts) needed for the capacitor plate assembly. Thus the D.C. voltage fed back to the capacitor plate assembly is determined by the transformer and (if phases are proper) will automatically be adjusted to make the transformer output very nearly zero.

The gain of amplifier (9) is varied simultaneously with the attenuation of (8). The reason for this is that if the gain of (9) were to remain fixed, the loop gain of the system would vary with the setting of (8). To avoid this, the gain of (9) is increased as the attenuation of (8) is increased, and decreased as the attenuation is decreased. Thus the ratio of the attenuation of (8) and the gain of (9) remains fixed on all ranges except the most sensitive, on which range the loop gain is down

a factor of ten.

The drive for the transducer is provided by power amplifier (5) which is driven by oscillator (19). The output of this oscillator is also applied, via phase shifter (18), as a reference to phase sensitive detector (17). The phase shifter allows the detector phase to be adjusted for maximum detector sensitivity.

A fraction of the D.C. feedback voltage (proportional to the magnetic moment of the sample) appears across the output of divider (11). This is applied to input A of chopper-stabilized amplifier (13). This is a differential amplifier whose output is in-phase with input A and whose output is zero, i.e., "at ground" when both inputs are at the same potential (regardless of any common potential). Inverse feedback is provided via divider (15) and variable D.C. source (12), the D.C. feedback voltage at input B being the sum of a fraction of the output determined by (15), and the output of the D.C. source (12). From the above discussion it will be seen that when the output of (12) is the same as that of (11), the output of (13),(14) will be at ground. If the D.C. output of the detector (17), i.e., the magnetic moment of the sample, should change slightly, a proportional change will occur at (14), the size of this change being determined by the setting of (15).

APPENDIX 2

DISCUSSION OF ERRORS

In this experiment, the significant measured quantities were the sample signal, the magnetic field, the mass of the sample, and the thermocouple emf. It is the purpose of this appendix to establish limits of accuracy for these measurements.

A. Magnetometer

1. Differential Sensitivity :

The system will detect a minimum change in the magnetic moment of 5×10^{-5} emu (corresponding to a change in magnetic susceptibility of 5×10^{-9} emu for a 1 cc sample in a 10^4 gauss magnetic field).

2. Stability :

Stability of the output signal is better than 1 part in 10^4 per day for a fixed coil geometry and magnetic field.

3. Absolute Accuracy :

Less than 2%.

4. Relative Accuracy :

Less than 1 %.

5. Reproducibility :

Less than 1 %.

B. Thermocouple

Thermal and contact emf's at low temperatures introduce a zero error in the thermocouple. At 4.2°K, the thermocouple emf is not zero and hence a correction is made before the thermocouple calibration is applied. At liquid helium temperature, the absolute error in the thermocouple emf is .005 millivolts. This corresponds to an absolute error in the temperature of 0.3°K. At 100°K, the absolute error in the thermocouple emf is .015 millivolts, corresponding to an absolute error in the temperature of 0.07°K.

The temperature measuring junction of the thermocouple is separated from the sample cavity by a few millimeters. There is then the possibility that the sample temperature is not that indicated by the thermocouple. The error from this source is estimated to be of the order of a few degrees.

The large scatter in the magnetic susceptibility versus 1000/T curve is due principally to the lack of sensitivity of the copper-constantan thermocouple at low temperatures.

C. Magnetic Field

The absolute error in the magnetic field using the NMR calibration as described in section 3.4, is 0.05 gauss.

D. Mass of the Sample

The absolute error in the mass of the sample of CsTi Alum is 0.05 milligrams.

E. Magnetic Susceptibility

The experimental magnetic susceptibility is a function of sample signal, sample mass, and magnetic field. The maximum possible error in the experimental magnetic susceptibility is 1.3 %.

BIBLIOGRAPHY

1. Azaroff,L.V.,Brophy,J.J., Electronic Processes in Metals. New York: McGraw-Hill Book Co., 1963.
2. Ballhausen,C.J., Introduction to Ligand Field Theory. New York: McGraw-Hill Book Co., 1962.
3. Bates,L.F., Modern Magnetism. London: Cambridge Univ. Press, 1961.
4. Benzie,R.J.,Cooke,A.H., Proc.Roy.Soc. (London), A209, 269,1951.
5. Bleaney,B.,Bogle,G.S.,Cooke,A.H.,Duffas,R.J.,O'Brien, M.C.M.,Stevens,K.W.H., Proc.Roy.Soc. (London), A68, 57,1955.
6. Bose,A.,Chakravarty,A.S.,Chatterjee,R., Indian J.Phys., 33,325,1959.
7. Bozorth,R.M., Ferromagnetism. New York: Van Nostrand, 1951.
8. Casimir,H.B.G., Magnetism and Very Low Temperatures. New York: Dover Publications,Inc., 1961.
9. Danan,H.,Herr,A.,Meyer,J.P., J.Applied Phys.,39,669, 1968.
10. de Haas,W.J.,Wiersma,E.C., Physica,2,438,1935.
11. de Haas,W.J.,Wiersma,E.C., Physica,3,491,1936.
12. de Haas,W.J.,du Pre,F.K., Physica,5,501,969,1938.
13. Dionne,G.F., Ph.D. thesis (unpublished),McGill Univ., 1964.

14. Dutta-Roy,S.K.,Chakravarty,A.S.,Bose,A.,Indian J.Phys., 33,483,1959.

15. Figgis,B.N.,Lewis,J.,Mabbs,F.,J.Chem.Soc.,2473,1963.

16. Foner,S.,Rev. Sci. Instr.,30,7,548,1959.

17. Gladney,H.M.,Swalen,J.D.,J.Chem.Phys.,42,6,1999,1965.

18. Gorter,C.J.,Teunissen,P.,Dijkestra,L.J.,Physica,5,1013, 1938.

19. Handel,J.Van den, thesis,Leiden Univ.,1940.

20. Kamimura,H.,J.Phys.Soc.Japan,11,1171,1956.

21. Kittel,C.,Introduction to Solid State Physics. New York: John Wiley and Sons Inc.,1967.

22. Kuo,S.S.,Numerical Methods and Computers. Reading, Massechusetts: Addison-Wesley Publishing Co.,1966.

23. Low,W.,Paramagnetic Resonance in Solids. New York: Academic Press,1960.

24. MacKinnon,J.A., M.Sc. thesis (unpublished),McGill Univ.,1963.

25. MacKinnon,J.A., Ph.D. thesis (unpublished),McGill Univ.,1968.

26. MacKinnon,J.A.,Raudorf,T., (unpublished work),McGill Univ.,1968.

27. Maartense,I., (unpublished work),McGill Univ.,1963.

28. Pake,G.E.,Paramagnetic Resonance. New York: W.A. Benjamin Inc.,1962.

29. Powell,R.L.,Caywood Jr.,L.P.,Bunch,M.D.,Low Temperature Thermocouples., Vol.II of Temperature,Its Measurement and Control in Science and Industry. ed.C.M.Hertzfeld, New York: Reinhold Publishing Co., 1962,p.65.

30. Rozenberg,H.M.,Low Temperature Solid State Physics. London: Oxford Univ. Press,1965.

31. Sygush,J., (unpublished work),McGill Univ.,1969.

32. Van Vleck,J.H.,J.Chem.Phys.,7,61,1939.

33. Van Vleck,J.H.,Phys.Rev.,57,426,1940.

34. Van Vleck,J.H.,Electric and Magnetic Susceptibilities. London: Oxford Univ. Press,1932.

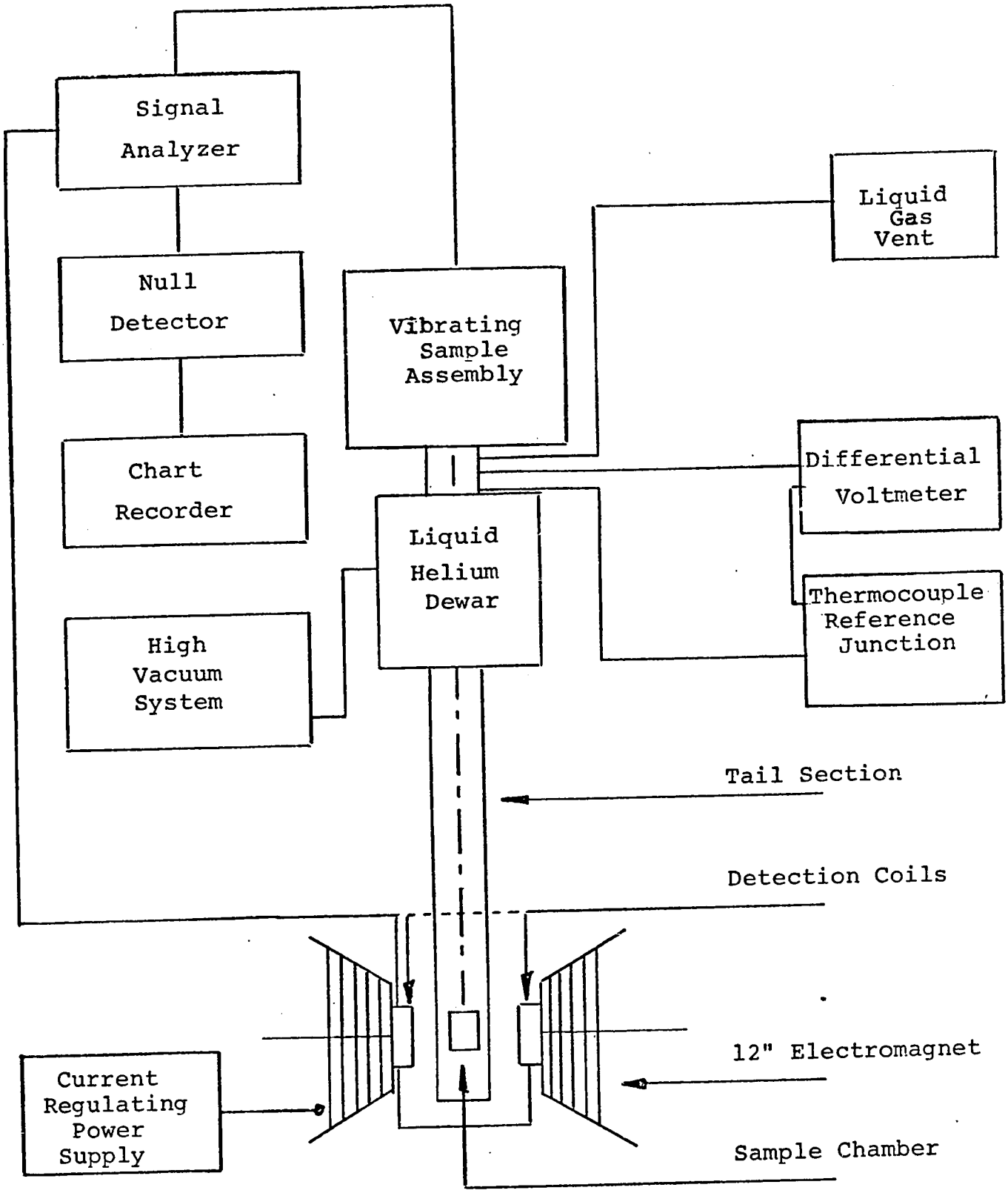

Fig. # 1. Block diagram of magnetic susceptibility experiment.

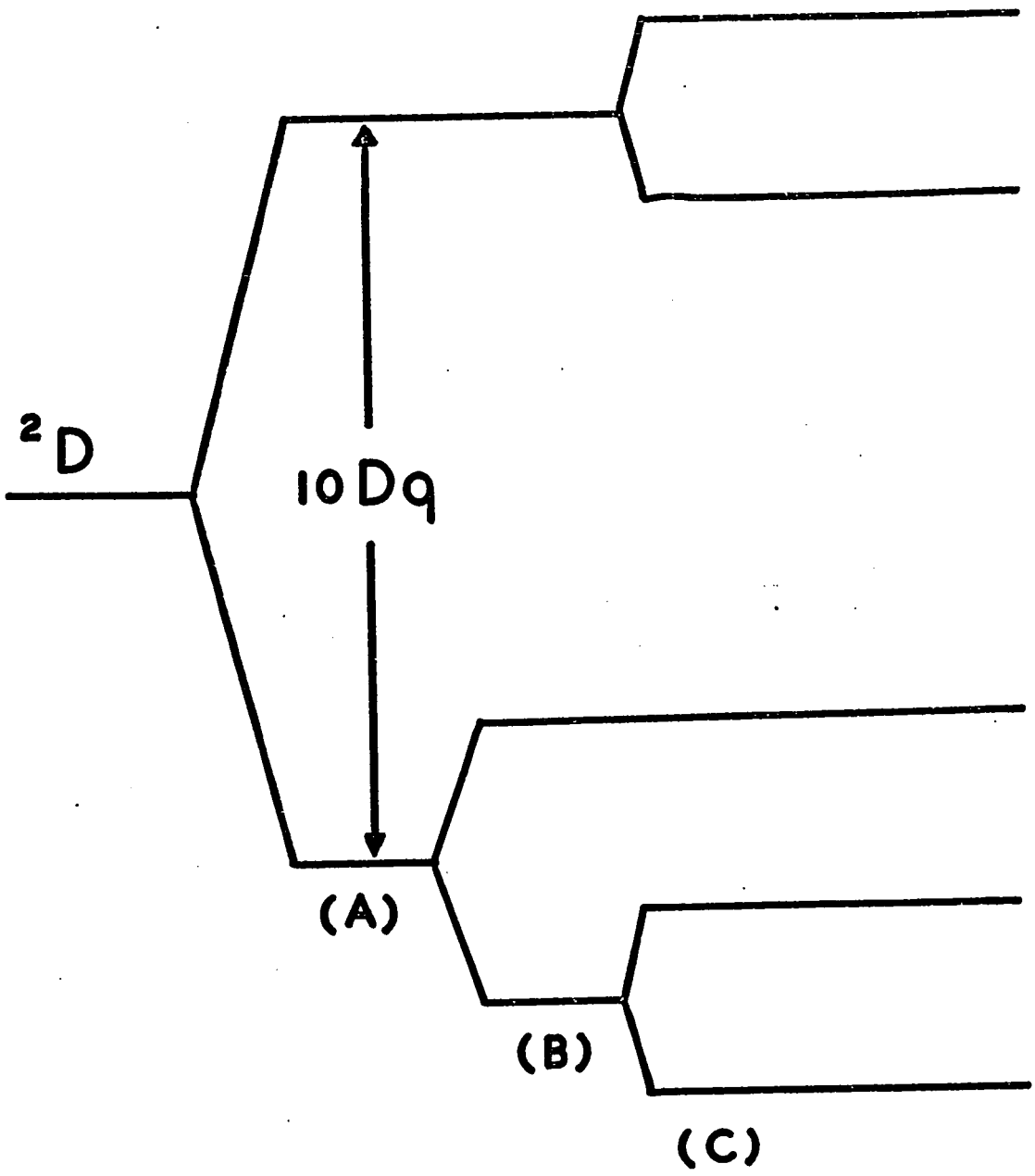

(A) CUBIC FIELD

(B) TRIGONAL DISTORTION

(C) SPIN-ORBIT COUPLING

Fig. # 2. Energy level diagram of Ti ion in CsTi Alum.

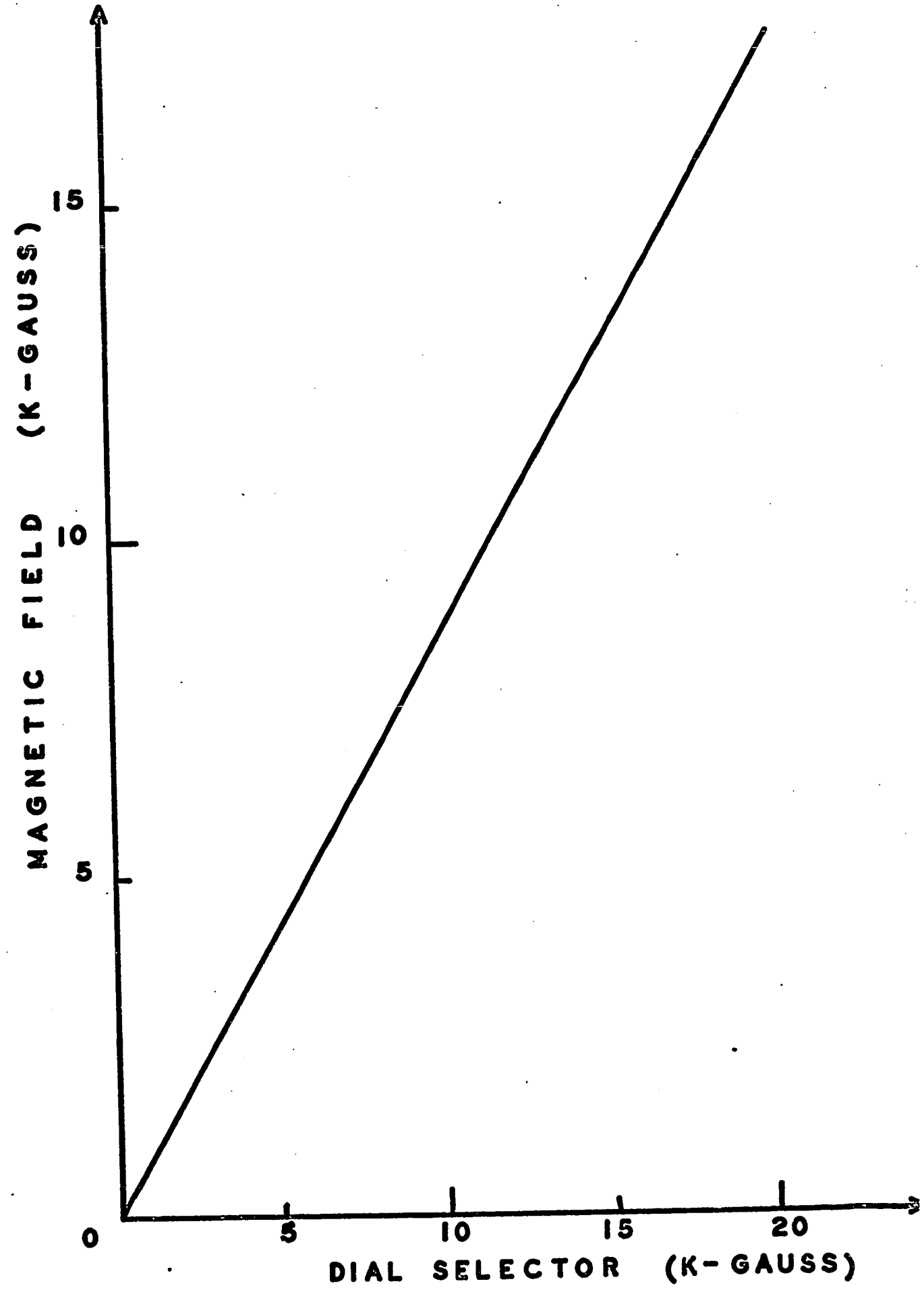

Fig. # 3. Calibration curve of 12" Electro magnet.

Reference for Fig.#4.

Components of the Electronic

Detection System

1. A.C. power output for divider transducer
2. Reference signal output
3. Sample signal output
4. D.C. feedback output
5. A.C. power amplifier
6. Reference pre-amplifier
7. Phase shifter # 1
8. Reference attenuator
9. Variable gain amplifier
10. Summing transformer
11. Precision voltage divider
12. Precision variable D.C. voltage source
13. Chopper-stabilized D.C. amplifier
14. Output to front panel null detector and external recorder
15. Null sensitivity control
16. D.C. amplifier
17. Phase sensitive detector
18. Phase shifter # 2
19. Sinusoidal oscillator

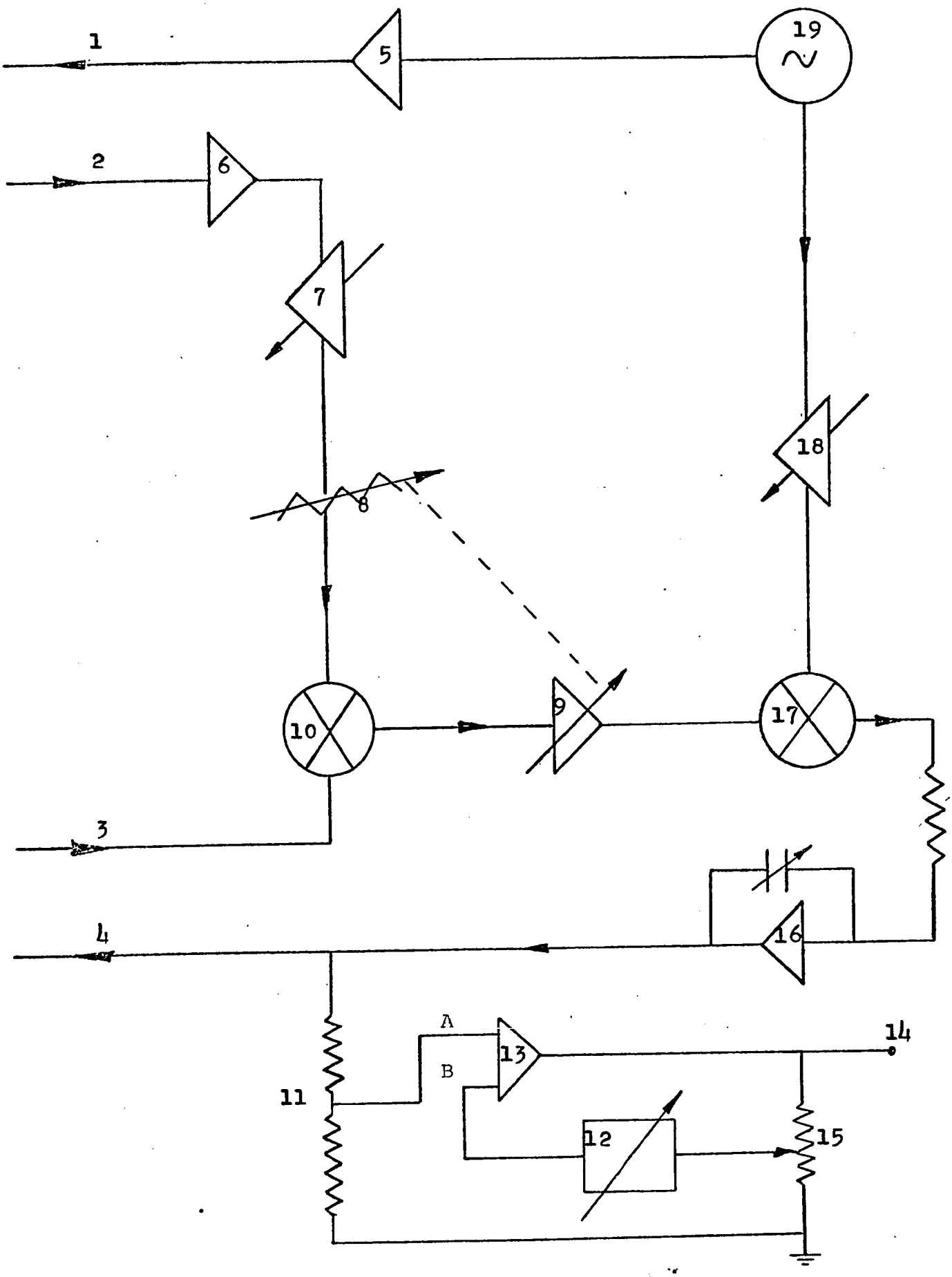

Fig.# 4: Detection system of the Magnetometer.

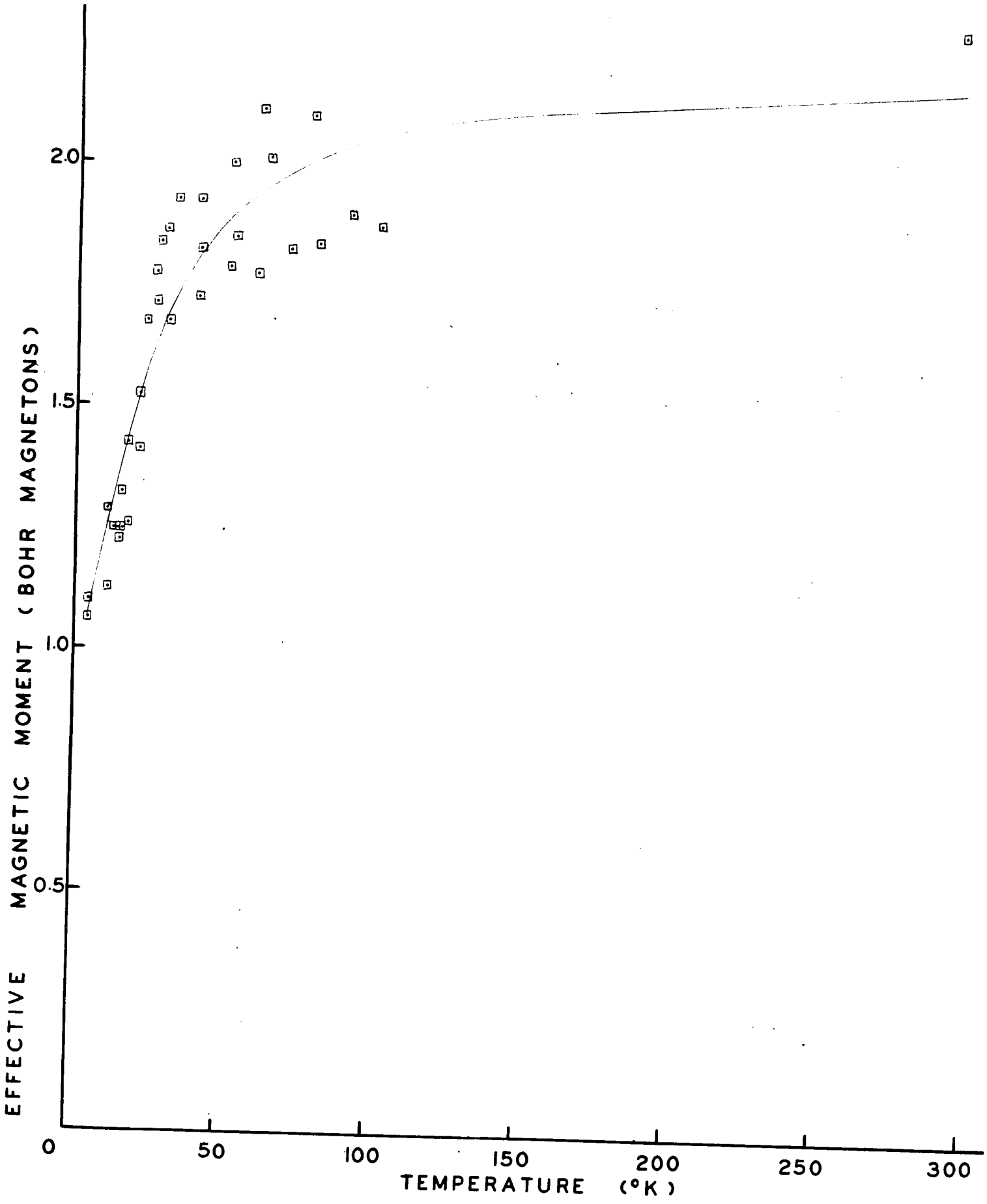

Fig. # 5. Effective Magnetic Moment versus Temperature

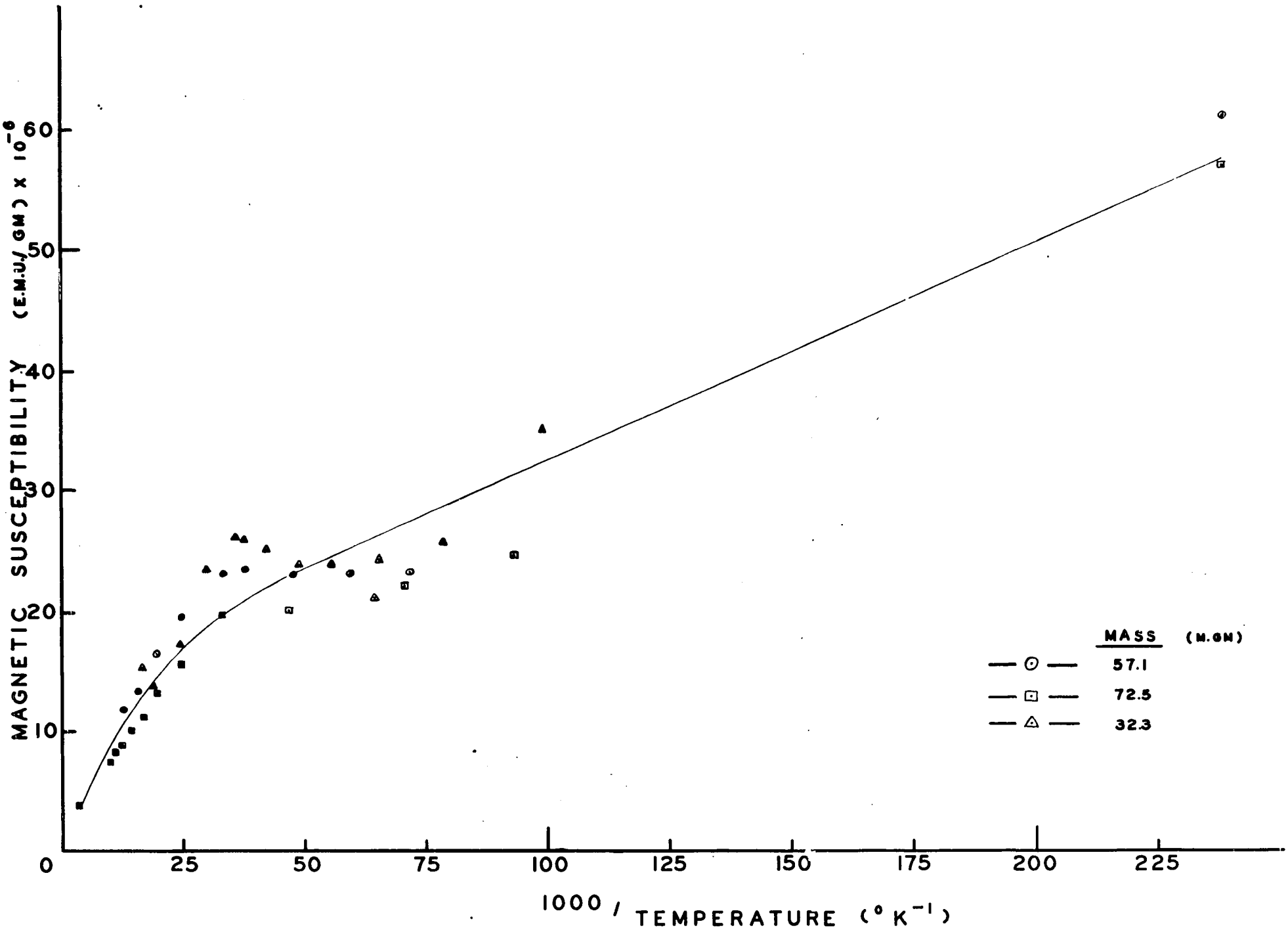

Fig. # 6. Magnetic Susceptibility versus 1000/T

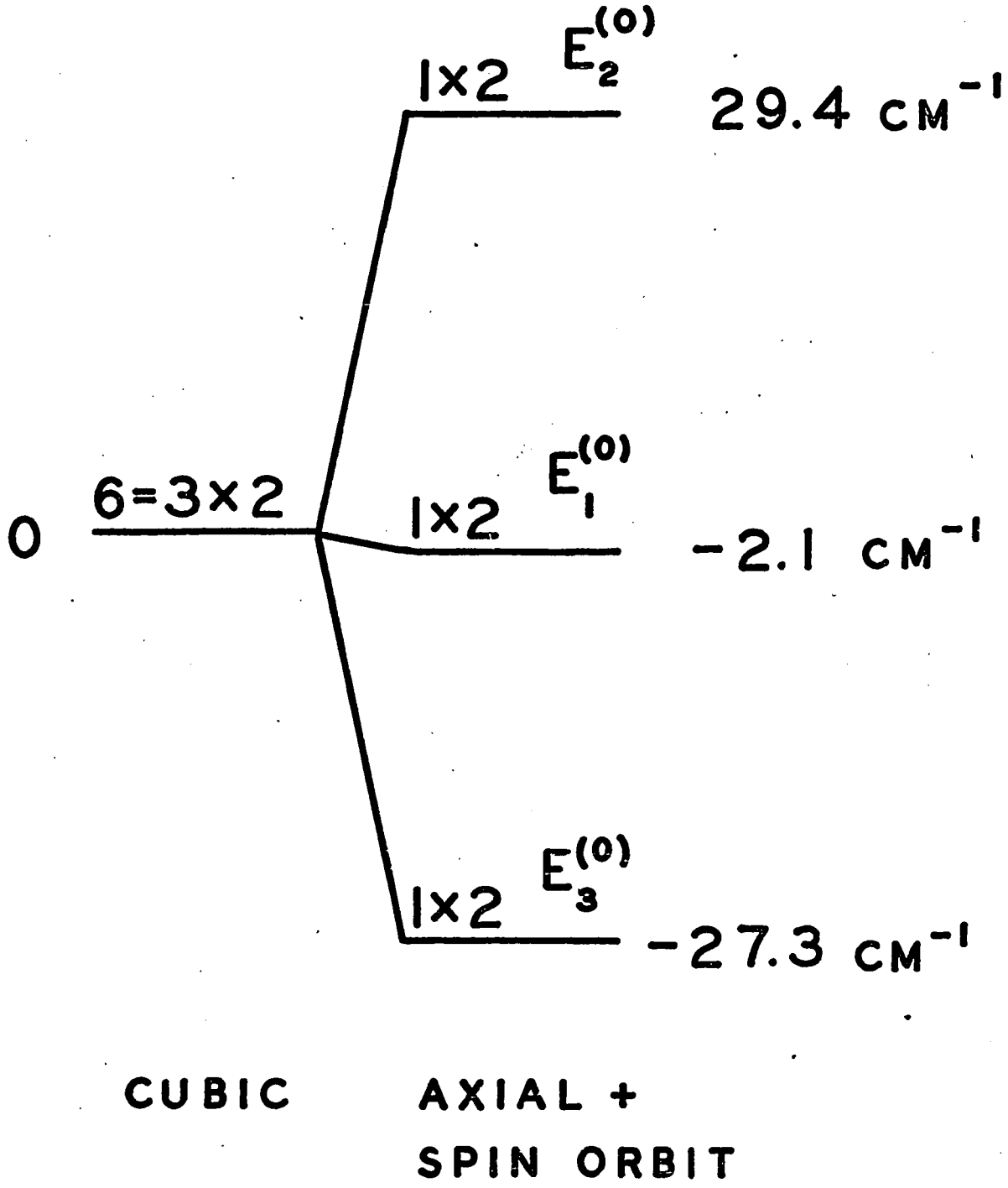

Fig. # 7. Experimental results of energy level calculations

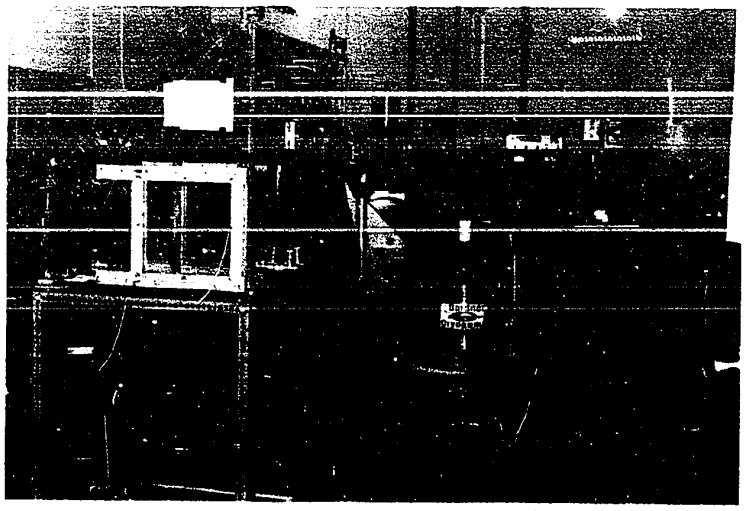

Fig. # 8. General view of Laboratory

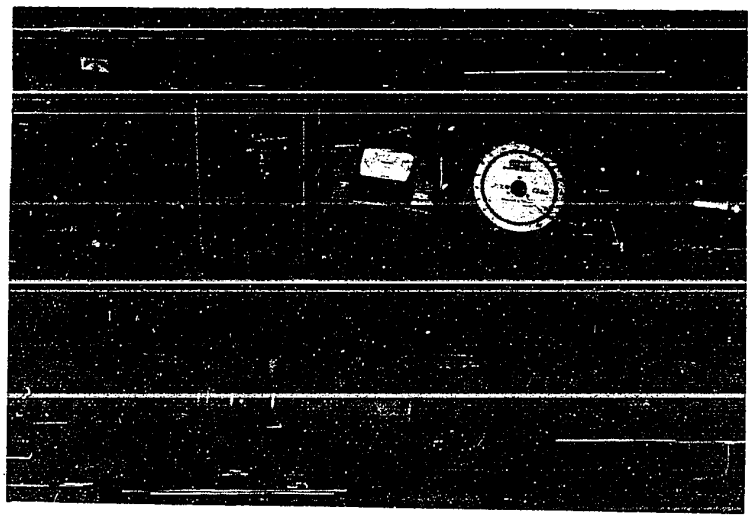

Fig. # 9. Experimental set up

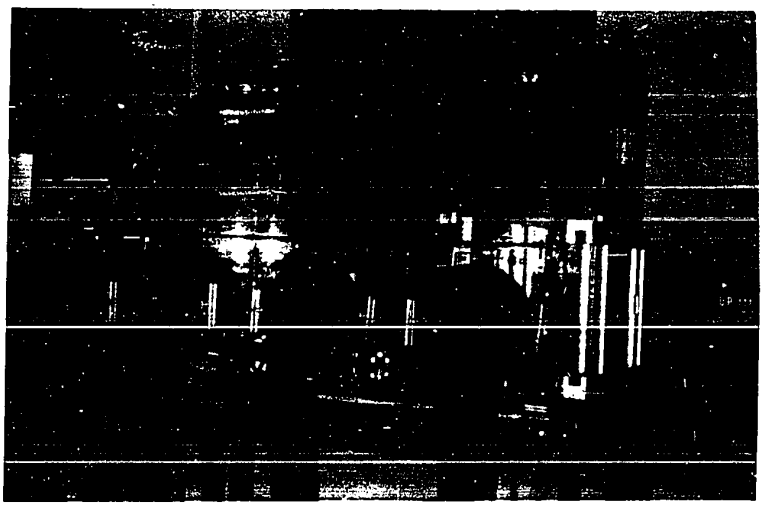

Fig. # 10. Glove box used in preparation of crystals